Voronoi Diagrams from Distance Graphs *

Mario Kapl† Franz Aurenhammer‡ Bert Jüttler†

Abstract

We present a new type of Voronoi diagram in $\mathbb{R}^2$ that respects the anisotropy exerted on the plane by a given distance graph. It is based on a metric obtained by smoothly and injectively embedding of $\mathbb{R}^2$ into $\mathbb{R}^m$, and a scalar-valued function for re-scaling the distances.

A spline representation of the embedding surface is constructed with the Gauß-Newton algorithm, which approximates the given distance graph in the sense of least squares. The graph is required to satisfy the generalized polygon inequality.

We explain a simple method to compute the Voronoi diagrams for such metrics, and give conditions under which Voronoi cells stay connected. Several examples of diagrams resulting from different metrics are presented.

1 Introduction

The Voronoi diagram of a given set of sites is a powerful and popular concept in geometry which possesses a wide range of applications, e.g. to motion planning, geometrical clustering and meshing [2]. Beside the classical Euclidean Voronoi diagram there exists a large number of generalizations of this structure.

Two examples relevant for the present note are the anisotropic Voronoi diagrams described in [7] and [9]. For each point p (say in $\mathbb{R}^2$), a different metric is defined which specifies the distances to all other points, as seen from p. However, the distance between two arbitrary points does *not* define a metric, because either the triangle inequality or the symmetry is violated. This is no serious hinderance for computing the anisotropic Voronoi diagram, though.

A different approach is followed in [8]. A Voronoi diagram on a parametric surface is generated, by taking geodesic distances between the points on the surface. The corresponding structure in the parameter domain of the surface is a Voronoi diagram which is possibly anisotropic. The computation of this type of diagram is rather expensive, as geodesic distances have to be computed frequently.

In this note we introduce a new metric framework on $\mathbb{R}^2$, called scaled embedding-generated (SEG) metrics, and use it to define a class of anisotropic Voronoi diagrams. It is based on a smooth one-to-one embedding of $\mathbb{R}^2$ into $\mathbb{R}^m$, for $m \geq 2$, and a scalar-valued scaling function. The construction of SEG metric Voronoi diagrams has several advantages. We have only one distance function for all points, which indeed defines a metric on $\mathbb{R}^2$, and the computation of distances is fast and simple. Also, some properties of such diagrams can be derived from the properties of the Euclidean Voronoi diagram in $\mathbb{R}^2$ and $\mathbb{R}^3$.

2 Preliminaries

We recall some basic concepts needed in the subsequent considerations.

Definition 1 The *medial axis* of a set $\mathbf{X} \subset \mathbb{R}^m$ is the (closure of the) set of all points in $\mathbb{R}^m$ that have at least two closest points in $\mathbf{X}$.

Definition 2 [1, 6] The *local feature size* at a point $\mathbf{p} \in \mathbf{X}$, denoted by $\mathrm{LFS}(\mathbf{p})$, is the Euclidean distance from $\mathbf{p}$ to the nearest point of the medial axis of $\mathbf{X}$.

Definition 3 [1, 6] Let $\mathbf{P_x} = \{\mathbf{x}_1, \mathbf{x}_2, \ldots\}$ be a finite subset of $\mathbf{X}$. We call $\mathbf{P_x}$ an *ε-sample* of $\mathbf{X}$ if for each point $\mathbf{p} \in \mathbf{X}$ there is a sample point $\mathbf{x}_i \in \mathbf{P_x}$ with $||\mathbf{p} - \mathbf{x}_i|| \leq \varepsilon \cdot \mathrm{LFS}(\mathbf{p})$.

Definition 4 Let $\mathbf{P} = \{\mathbf{p}_1, \mathbf{p}_2, \ldots\}$ be a finite set of points (called sites) in $\mathbb{R}^m$. For a given metric D on $\mathbb{R}^m$, we define the *Voronoi cell* of a site $\mathbf{p}_i \in \mathbf{P}$ as the open set

$$V_D^i(\mathbf{P}) = \{\mathbf{p} \in \mathbb{R}^m \mid D(\mathbf{p}, \mathbf{p}_i) < D(\mathbf{p}, \mathbf{p}_j) \text{ for all } j \neq i\}.$$

The *Voronoi diagram* $V_D(\mathbf{P})$ is given by the complement of all Voronoi cells in $\mathbb{R}^m$,

$$V_D(\mathbf{P}) = \mathbb{R}^m \setminus \left(\bigcup_i V_D^i(\mathbf{P}) \right).$$

We denote the Voronoi diagram with respect to the Euclidean metric by $V(\mathbf{P})$. A Voronoi diagram is called *orphan-free* if all its Voronoi cells are connected. In the case of the Euclidean metric, the diagram is always orphan-free, because its regions are

*This work has been supported by the ESF EUROCORES Programme EuroGIGA - Voronoi, Austrian Science Foundation (FWF).

†Institute of Applied Geometry, Johannes Kepler University, Linz, Austria, {mario.kapl|bert.juettler}@jku.at

‡Institute for Theoretical Computer Science, University of Technology, Graz, Austria, auren@igi.tu-graz.ac.at.

This is an extended abstract of a presentation given at EuroCG 2013. It has been made public for the benefit of the community and should be considered a preprint rather than a formally reviewed paper. Thus, this work is expected to appear in a conference with formal proceedings and/or in a journal.

intersections of open halfspaces of $\mathbb{R}^m$, and thus are convex polyhedra.

3 The SEG metric framework

We now introduce the metric framework we would like to work with.

Definition 5 Let $\mathbf{x} : \mathbb{R}^2 \to \mathbb{R}^m$, for $m \geq 2$, be a continuous one-to-one embedding, with $\mathbf{x}(u,v) = (x_1(u,v), \ldots, x_m(u,v))$. In addition, let $r \mapsto d(r)$, for $r \geq 0$, be a scalar-valued scaling function with the following properties:

- $d(0) = 0$
- $d(r) > 0$, for $r > 0$
- $d'(r) \geq 0$, for $r \geq 0$
- $d(r)/r$ is monotonically decreasing, for $r > 0$

We define the distance D between two points $\mathbf{u}_1 = (u_1, v_1)$ and $\mathbf{u}_2 = (u_2, v_2)$ in $\mathbb{R}^2$ as

$$D(\mathbf{u}_1, \mathbf{u}_2) = d(||\mathbf{x}(u_1, v_1) - \mathbf{x}(u_2, v_2)||). \qquad (1)$$

Theorem 6 *The distance D given by* (1) *defines a metric on $\mathbb{R}^2$.*

Proof. For all $\mathbf{u}_1, \mathbf{u}_2, \mathbf{u}_3 \in \mathbb{R}^2$, the distance D has to satisfy the following conditions:

(i) $D(\mathbf{u}_1, \mathbf{u}_2) \geq 0$,
(ii) $D(\mathbf{u}_1, \mathbf{u}_2) = 0$ iff $\mathbf{u}_1 = \mathbf{u}_2$,
(iii) $D(\mathbf{u}_1, \mathbf{u}_2) = D(\mathbf{u}_2, \mathbf{u}_1)$, and
(iv) $D(\mathbf{u}_1, \mathbf{u}_3) \leq D(\mathbf{u}_1, \mathbf{u}_2) + D(\mathbf{u}_2, \mathbf{u}_3)$.

Conditions (i) and (iii) are trivially fulfilled. To show condition (ii), we have to use the fact that the embedding $\mathbf{x}(u,v)$ has no self-intersections, since the map $\mathbf{x} : \mathbb{R}^2 \to \mathbb{R}^m$ is one-to-one. The triangle inequality (iv) remains to be shown. For the sake of brevity we denote the Euclidean distance $||\mathbf{x}(\mathbf{u}_i) - \mathbf{x}(\mathbf{u}_j)||$ by $l_{i,j}$. Since the Euclidean metric satisfies the triangle inequality, we have

$$l_{1,3} \leq l_{1,2} + l_{2,3}.$$

Now we distinguish two cases.
Case 1: $(l_{1,3} \leq l_{1,2})$ or $(l_{1,3} \leq l_{2,3})$.
Since $d'(r) \geq 0$ for $r \geq 0$ we have

$$d(l_{1,3}) \leq d(l_{1,2}) \text{ or } d(l_{1,3}) \leq d(l_{2,3}),$$

$$d(l_{1,3}) \leq d(l_{1,2}) + d(l_{2,3}).$$

This shows the triangle inequality (iv).
Case 2: $l_{1,3} > l_{1,2}$ and $l_{1,3} > l_{2,3}$.
Since $d(r)/r$ is monotonic decreasing we know that

$$\frac{d(l_{1,3})}{l_{1,3}} \leq \frac{d(l_{1,2})}{l_{1,2}} \text{ and } \frac{d(l_{1,3})}{l_{1,3}} \leq \frac{d(l_{2,3})}{l_{2,3}}.$$

Now we have

$$\begin{aligned} d(l_{1,2}) + d(l_{2,3}) &= l_{1,2}\frac{d(l_{1,2})}{l_{1,2}} + l_{2,3}\frac{d(l_{2,3})}{l_{2,3}} \geq \\ &\geq l_{1,2}\frac{d(l_{1,3})}{l_{1,3}} + l_{2,3}\frac{d(l_{1,3})}{l_{1,3}} = (l_{1,2} + l_{2,3})\frac{d(l_{1,3})}{l_{1,3}} \geq \\ &\geq l_{1,3}\frac{d(l_{1,3})}{l_{1,3}} = l_{1,3}, \end{aligned}$$

which proves the triangle inequality (iv). □

We will call D the *scaled embedding-generated (SEG) metric* in the sequel. For $m = 2$ or $m = 3$, the embedding $\mathbf{x}(u,v)$ is a parametric surface without self-intersections in $\mathbb{R}^2$ and $\mathbb{R}^3$, respectively. Two examples of possible scaling functions are

$$d(r) = ar \quad \text{or} \quad d(r) = a\ln(br + 1) \qquad (2)$$

for suitable constants $a, b > 0$.

With the help of the metric D, we can define generalized disks with radius $r > 0$ and center $\mathbf{c} \in \mathbb{R}^2$,

$$B_r(\mathbf{c}) = \{\mathbf{p} \in \mathbb{R}^2 \mid D(\mathbf{p}, \mathbf{c}) \leq r\}.$$

Clearly, for embedding dimension $m = 2$, these disks are topological disks, by the properties of $\mathbf{x}(u,v)$. Moreover, we have:

Lemma 7 *Let $m = 3$, $\mathbf{c} \in \mathbb{R}^2$, and $\bar{r} = d^{-1}(r)$. If $\bar{r} < LFS(\mathbf{x}(\mathbf{c}))$, then the disks $B_r(\mathbf{c})$ are topological disks (and generalized circles are topological circles).*

4 Fitting SEG metrics to distance graphs

We now explain a method for computing suitable SEG metrics. The idea is to construct a spline embedding $\mathbf{x}(u,v)$ which approximates a given *distance graph* G on n points in the unit square $[0,1]^2$ of the parameter domain $\mathbb{R}^2$.

To achieve high accuracy in the approximation, we require G to satisfy the *generalized polygon inequality*, that is, for each edge (p,q) the associated length $L_{p,q}$ is at most the length of any existing path in G from p to q.

For simplicity, the scaling function is temporarily set to the identity, $d(r) = r$.

We will construct an embedding surface $\mathbf{x}(u,v) = (x_1(u,v), \ldots, x_m(u,v))$ with $m \geq 3$, where the first two coordinate functions are the linear functions $x_1(u,v) = c^{(1)}\, u$ and $x_2(u,v) = c^{(2)}\, v$. The remaining coordinate functions $x_i(u,v)$ for $i \geq 3$ are given by B-spline functions of degree (p_1, p_2),

$$x_i(u,v) = \sum_{j=0}^{n_1}\sum_{k=0}^{n_2} c_{j,k}^{(i)} M_j^{p_1}(u) N_k^{p_2}(v)$$

with $c_{j,k}^{(i)} \in \mathbb{R}$. The basic functions $(M_j^{p_1}(u))_{j=0,\ldots,n_1}$ and $(N_k^{p_2}(u))_{k=0,\ldots,n_2}$ are B-splines of degree (p_1, p_2)

with respect to the open knot sequences $\mathcal{S} = (s_j)_{j=0,\ldots,n_1+p_1+1}$ and $\mathcal{T} = (t_k)_{k=0,\ldots,n_1+p_1+1}$, respectively. Now we compute the unknown coefficients $\mathbf{c} = (c^{(1)}, c^{(2)}, c^{(3)}_{0,0}, \ldots, , c^{(3)}_{n_1,n_2})$ by solving the minimization problem

$$\mathbf{c} = \arg\min \sum_{(p,q)\in G} \Big(\underbrace{||\mathbf{x}(p) - \mathbf{x}(q)||^2 - L^2_{p,q}}_{R_{p,q}(\mathbf{c})} \Big)^2.$$

Since this optimization problem is non-linear and the objective function is a sum of squares, we use the Gauß-Newton algorithm to solve it. For each iteration step, we minimize the objective function

$$\Big(\sum_{(p,q)\in G} (R_{p,q}(\mathbf{c}^0) + \nabla R_{p,q}(\mathbf{c}^0)(\Delta\mathbf{c} - \mathbf{c}^0))^2 \Big) + \omega||\Delta\mathbf{c} - \mathbf{c}^0||^2, \quad (3)$$

which includes a Tikhonov regularization term, with respect to $\Delta\mathbf{c}$.

In the objective function (3), the vector $\mathbf{c}^0$ denotes the solution from the last step, $\Delta\mathbf{c}$ is the update, and $\nabla R_{p,q}$ is the row vector given by the partial derivatives of $R_{p,q}$ with respect to the control points $\mathbf{c}_{j,k}$. In addition, $\omega > 0$ is the parameter for the Tikhonov regularization term.

The obtained embedding $\mathbf{x}(u, v)$ has no self-intersections, as long as none of the coefficients $c^{(1)}$ and $c^{(2)}$ becomes zero in the optimization process. To avoid this case, or the case that one of them is close to zero, we allow the user to specify these coefficients in our implementation. We have used this approach in all the examples presented below.

The use of the two linear functions above can be seen as some kind of regularization. By using sufficiently small coefficients $c^{(1)}$ and $c^{(2)}$ (combined with a sufficiently large dimension of the embedding), one can minimize the influence of this regularization while still avoiding self-intersections of the embedding. The remaining coefficients $c^{(i)}_{j,k}$ of the initial solutions were chosen randomly from the interval $[-\frac{1}{10}, \frac{1}{10}]$.

Note that different initial solutions give different results. In our experience, however, the obtained different solutions were approximations of similar quality of the distance graph G. Moreover, we noticed that for most of our tested distance graphs an embedding of $\mathbb{R}^2$ into $\mathbb{R}^m$ for $m \in \{3, 4, 5\}$ leads to a satisfactory result. It seems, that as long as the generalized polygon inequality is fulfilled, the distance graph is usually 'almost exactly' approximated by the produced embedding. But especially in the case of a distance graph with a high valency for each point, an embedding into a higher dimension could probably be needed.

The resulting embedding $\mathbf{x}(u, v)$ induces an SEG metric on the unit square $[0, 1]^2$. By extending this restricted embedding to a continuous one-to-one embedding $\mathbf{x} : \mathbb{R}^2 \to \mathbb{R}^m$, we obtain an SEG metric on $\mathbb{R}^2$, which accurately approximates a given distance graph.

5 SEG metric Voronoi diagrams

We will now use the metric D in (1) to construct a respective Voronoi diagram in $\mathbb{R}^2$, in a simple way.

Let $\mathbf{P} = \{\mathbf{u}_1, \mathbf{u}_2, \ldots\}$ be a set of sites in $\mathbb{R}^2$. The SEG metric Voronoi diagram $V_D(\mathbf{P})$ for D can be generated in the following way. Given the sites $\mathbf{u}_i \in \mathbb{R}^2$, we first calculate the corresponding points $\mathbf{x}_i = \mathbf{x}(\mathbf{u}_i)$ on the embedding $\mathbf{x}(u, v)$, which has been used to define D. Then we compute, for the obtained set of points $\mathbf{P}_\mathbf{x} = \{\mathbf{x}_1, \mathbf{x}_2, \ldots\}$ in $\mathbb{R}^m$, their Euclidean Voronoi diagram $V(\mathbf{P}_\mathbf{x})$. By intersecting the resulting Voronoi cells with the embedding surface $\mathbf{x}(u, v)$, we obtain a Voronoi diagram on $\mathbf{x}(u, v)$, which defines for the corresponding parameter values $(u, v) \in \mathbb{R}^2$ the desired SEG metric Voronoi diagram $V_D(\mathbf{P})$ in $\mathbb{R}^2$.

This approach is similar to that in [3], who showed that the anisotropic Voronoi diagram of [9] can be obtained by intersecting a so-called power diagram in $\mathbb{R}^5$ with a suitable surface. (Power diagrams are generalized Voronoi diagrams whose cells are still convex polyhedra; see e.g. [2].)

Before giving examples of SEG metric Voronoi diagrams constructed with our approach, let us consider some conditions under which $V_D(\mathbf{P})$ is orphan-free. Disconnectedness of a Voronoi cell in $V_D(\mathbf{P})$ means that the corresponding m-dimensional polyhedral cell in the Euclidean Voronoi diagram intersects the embedding surface more than once.

Clearly, $V_D(\mathbf{P})$ is orphan-free in the case $m = 2$, since $\mathbf{x}(u, v)$ then is a smooth one-to-one embedding into $\mathbb{R}^2$, and the Euclidean Voronoi diagram is always orphan-free. We further have:

Lemma 8 *Let $m = 3$, and assume that $\mathbf{x}(u, v)$ is C^2-smooth. If the set of sites $\mathbf{x}(\mathbf{P})$ is a 0.18-sample of the surface $\mathbf{X} = \mathbf{x}(\mathbb{R}^2)$, then the resulting diagram $V_D(\mathbf{P})$ is orphan-free.*

Proof. It is sufficient to show that each Voronoi cell $V^i(\mathbf{P}_\mathbf{x})$ of the Euclidean Voronoi diagram $V(\mathbf{P}_\mathbf{x})$ in $\mathbb{R}^3$ intersects the embedding $\mathbf{x}(u, v)$ in a topological disk. Since $\mathbf{x}(u, v)$ is a C^2-smooth embedding into $\mathbb{R}^3$, and $\mathbf{x}(\mathbf{P})$ is a 0.18-sample of $\mathbf{X}$, we can apply Lemma 3.10 in [6], which exactly states the desired fact. □

6 Examples

Consider the two distance graphs shown in Figure 1. For both graphs we have constructed embeddings into $\mathbb{R}^3$. Voronoi diagrams have been generated for the resulting approximating SEG metrics, for a set of uniformly distributed sites.

Two more involved distance graphs are depicted in Figure 2. To obtain SEG metrics with accurrate approximations, we have generated spline embeddings into $\mathbb{R}^5$ and $\mathbb{R}^7$, respectively. The obtained SEG metric Voronoi diagrams are shown for a set of uniformly

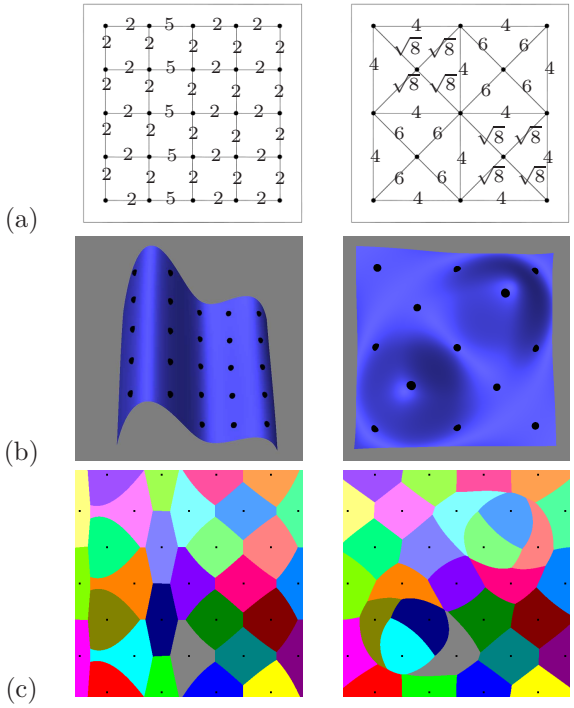

Figure 1: (a) Distance graphs; (b) Embeddings into $\mathbb{R}^3$; (c) Examples of SEG metric Voronoi diagrams.

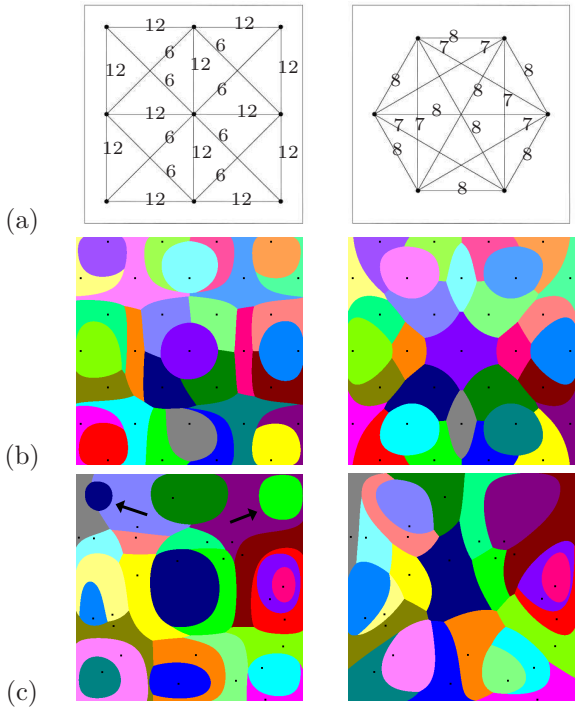

Figure 2: (a) Distance graphs; (b) and (c) Examples of SEG metric Voronoi diagrams.

distributed sites in (b), and for a set of non-uniformly distributed sites in (c). Occurring orphans are indicated by arrows.

7 Conclusion

We have introduced the concept of scaled embedding-generated (SEG) metrics, and have studied some of their properties. SEG metrics are a versatile tool for reflecting the anisotropy specified by distance graphs in the plane. Also, they lead to a new type of generalized Voronoi diagram in $\mathbb{R}^2$ in a canonical way.

As a possible application of our framework, we could generate a metric, which gives us the time of travel between cities. For the construction of the associated spline embedding, only a small number of selected times would be needed.

Various questions remain open, for example, conditions under which Voronoi cells are connected (or simply connected), if the embedding is in dimensions higher than 3; cf. the results in [4, 5]. In the non-orphan-free case, bounds on the number of connected Voronoi sub-cells are of interest.

Instead of the Voronoi diagram, also the medial axis for shapes with respect to the generalized disks defined by the new metric is worth studying.

References

[1] N. Amenta, S. Choi, and R.K. Kolluri. The power crust, unions of balls, and the medial axis transform. *Computational Geometry: Theory and Applications* 19 (2001), 127–153.

[2] F. Aurenhammer and R. Klein. Voronoi diagrams. In: J. Sack and G. Urrutia (eds.), *Handbook of Computational Geometry*, Elsevier, Amsterdam, 2000, 201–290.

[3] J.-D. Boissonnat, C. Wormser, and M. Yvinec. Anisotropic diagrams: Labelle Shewchuk approach revisited. *Theoretical Computer Science* 408 (2008), 163–173.

[4] G.D. Canas and S.J. Gortler. Orphan-free anisotropic Voronoi diagrams. *Discrete & Computational Geometry* 46 (2011), 526–541.

[5] G.D. Canas and S.J. Gortler. Duals of orphan-free anisotropic Voronoi diagrams are triangulations. *Proc. 28th Ann. Symposium on Computational Geometry*, 2012, 219–228.

[6] T.K. Dey. *Curve and Surface Reconstruction: Algorithms with Mathematical Analysis*. Cambridge Monographs on Applied and Computational Mathematics 23, Cambridge University Press, 2007.

[7] Q. Du and D. Wang. Anisotropic centroidal Voronoi tessellations and their applications. *SIAM Journal on Scientific Computing* 26 (2005), 737–761.

[8] R. Kunze, F.-E. Wolter, and T. Rausch. Geodesic Voronoi diagrams on parametric surfaces. *Proc. Conference on Computer Graphics International*, 1997, 230–237.

[9] F. Labelle and J.R. Shewchuk. Anisotropic Voronoi diagrams and guaranteed-quality anisotropic mesh generation. *Proc. 19th Ann. Symposium on Computational Geometry*, 2003, 191–200.